Liquid Crystals
Publication details, including instructions for authors and subscription information:
http://www.informaworld.com/smpp/title~content=t713926090

Determination of the difference of flexoelectric coefficients in a nematic liquid crystal using a conoscopic technique

E. K. Tidey[a]; L. A. Parry-Jones[a]; S. J. Elston[a]
[a] Department of Engineering Science, University of Oxford, Oxford, United Kingdom

To cite this Article Tidey, E. K. , Parry-Jones, L. A. and Elston, S. J.(2007) 'Determination of the difference of flexoelectric coefficients in a nematic liquid crystal using a conoscopic technique', Liquid Crystals, 34: 2, 251 — 255
To link to this Article: DOI: 10.1080/02678290601097342
URL: http://dx.doi.org/10.1080/02678290601097342

Liquid Crystals, Vol. 34, No. 2, February 2007, 251–255

Determination of the difference of flexoelectric coefficients in a nematic liquid crystal using a conoscopic technique

E. K. TIDEY, L. A. PARRY-JONES and S. J. ELSTON
Department of Engineering Science, University of Oxford, Parks Road, Oxford, OX1 3PJ, United Kingdom

(*Received 17 July 2006; accepted 23 October 2006*)

The conoscopic images of twisted nematic liquid crystal devices filled with E7 are analysed under the application of in-plane electric fields. The differences observed between the images for positive and negative applied fields are attributed to the flexoelectric effect. By comparison of the conoscopic images with theoretical predictions made using an extended Jones technique, the sign and magnitude of the difference between the splay and bend flexoelectric coefficients is determined for E7.

Flexoelectricity in nematic liquid crystals was predicted by Meyer in 1969 [1] and is the term used to describe the coupling between elastic distortions and molecular reorientation due to dielectric anisotropy. This effect has been of recent scientific interest due to two particular device technologies which rely on flexoelectricity for their operation. One uses flexoelectricity to achieve a high speed, analogue in-plane switching mode [2, 3, 4], whereas the other uses the effect to facilitate switching between two bistable states [5, 6].

According to Meyer [1], the total flexoelectric polarisation is:

$$\mathbf{P_f} = e_1(\nabla\cdot\mathbf{n})\mathbf{n} + e_3(\nabla\times\mathbf{n})\times\mathbf{n}, \quad (1)$$

and therefore consists of two separate contributions. One occurs in pear shaped molecules with a longitudinal dipole moment: here a splay deformation causes a net polarisation, with associated coefficient e_1. The other occurs in banana shaped moleculeswith a transverse dipole, and the coefficient e_3 is associated with the corresponding bend distortion. Different experimental geometries tend to probe these two modes in one of two ways [7]. For example, the analogue in-plane switching mode mentioned above is sensitive to the difference of the coefficients $e_1 - e_3$ [3], whereas the distortion of a HAN cell in response to an out-of-plane-field (for example) is sensitive to the sum e_1+e_3 [8]. This has the consequence that measurements tend to be of either the sum or the difference of the coefficients, and it is the latter which we will consider in this paper.

At present, the most commonly used method to determine the difference between the flexoelectric coefficients $e_1 - e_3$ is to measure the amount of twist produced in the optic axis of a cholesteric helix when subjected to an electric field normal to the helical axis [3, 4]. This effect, often referred to as the 'flexoelectro-optic' effect, was predicted in 1987 by Patel and Meyer [2], and forms the basis of the analogue in-plane switching mode referred to above. This measurement technique has the advantage of being very simple, provided that the material to be measured is chiral and easy to align in a uniform-lying-helix (ULH) texture. For difficult to align or achiral materials, we have proposed a method that uses an in-plane electric field to perturb a twisted nematic (TN) cell [9]. This geometry is effectively one quarter pitch of the cholesteric helix in the flexoelectric-optic effect, but rotated through 90°. We therefore see the same effect (described below) but with the advantage that it can be applied to any nematic liquid crystal, achiral or otherwise.

Consider a TN cell under the application of an applied in-plane electric field. The interaction of the electric field with the (positive) dielectric anisotropy of the liquid crystal will cause the director to rotate towards the direction of the applied field. In the approximation that the electric field can be considered to be exactly in the plane of the cell, i.e. parallel to the glass surfaces, then this effect will cause only a twist of the director, i.e. the director will remain everywhere parallel to the glass surfaces. If, however, we include the effects of flexoelectricity, then there will be some tilting of the director. This is entirely analogous to the twisting of the optic axis of a cholesteric liquid crystal in the flexoelectric optic effect. Figure 1 shows the predicted twist and tilt of the director in a TN cell with in-plane electric fields of $\pm 0.01\,\mathrm{V}/\mu\mathrm{m}$, in the case where the electric field is applied parallel to one of the rubbing directions (at a twist angle of 90° in this case). It is clear from part (a) that when there is no flexoelectric effect included, the distortion is pure twist, but that a tilt of up to 3° appears when the flexoelectric coupling is included. Note that in this case the tilt direction is opposite for the two signs of field. Part (b)

Liquid Crystals
ISSN 0267-8292 print/ISSN 1366-5855 online © 2007 Taylor & Francis
http://www.tandf.co.uk/journals
DOI: 10.1080/02678290601097342

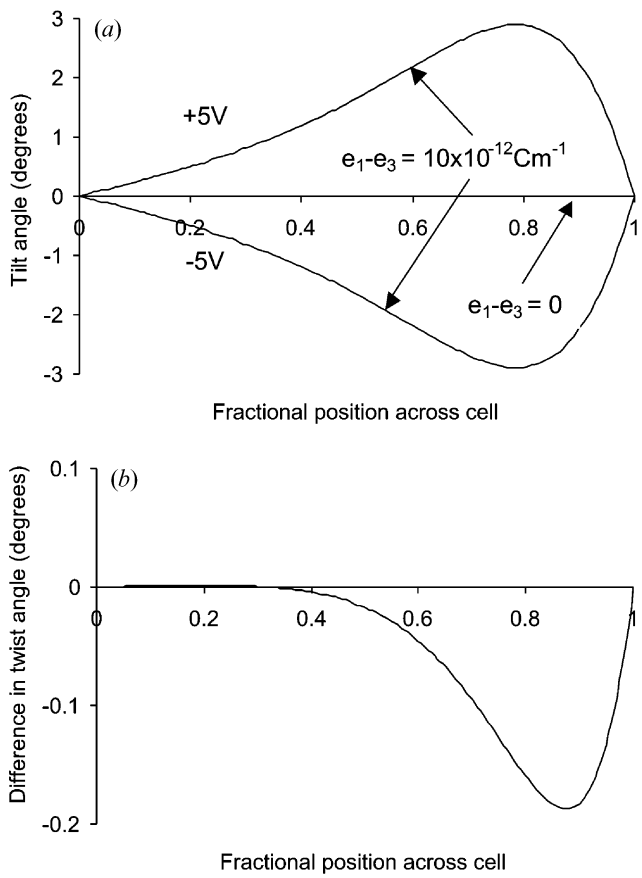

Figure 1. Theoretical predictions for the equilibrium director profile in a 100μm twisted nematic device under the application of in-plane electric fields of ± 0.01V/μm, for both zero flexoelectric coefficient and for $e_1 - e_3 = 10.0 \times 10^{-12}$Cm^{-1}. Part (a) shows the tilt component of the director: it is zero everywhere unless there is some flexoelectric coupling. Part (b), which shows the difference in the twist angle of the director with and with the flexoelectric effect,shows that the impact of flexoelectricity on the director twist is negligible.

shows that the twist profile of the director is hardly affected by flexoelectricity, at least in this case here where the applied electric field is relatively low.

These director profiles have been generated using a simple one-dimensional model of the nematic liquid crystal, minimising the following free energy expression:

$$
\begin{aligned}
F &= F_{\text{elastic}} + F_{\text{dielectric}} + F_{\text{flexoelectric}} \\
&= \frac{K_{11}}{2}(\nabla\cdot\mathbf{n})^2 + \frac{K_{22}}{2}\left(\mathbf{n}\cdot\nabla\times\mathbf{n} - \frac{2\pi}{p_0}\right)^2 + \frac{K_{33}}{2}((\nabla\times\mathbf{n})\times\mathbf{n})^2 \\
&\quad - \frac{1}{2}\varepsilon_0\Delta\varepsilon(\mathbf{n}\cdot\mathbf{E})^2 - (e_1(\nabla\cdot\mathbf{n})\mathbf{n} + e_3(\nabla\times\mathbf{n})\times\mathbf{n})\cdot\mathbf{E}
\end{aligned} \tag{2}
$$

where the director angle is allowed to vary across the thickness of the cell only (along z), and the electric field applied is in a direction exactly perpendicular to that (along y). This is a very good approximation to the true experimental situation, as explained below. The anchoring conditions at the boundaries are assumed to be infinitely strong, that is, the director cannot move at the two surfaces.

In our previous work [9], our experimental measurements of the flexoelectrically induced tilt were made by observing off axis transmission between crossed polarisers, at two specific angles of incidence. As the applied electric field was increased from zero, the signal in one detector increased as the other decreased, and this was reversed for the opposite direction of electric field. Here we were successful in determining $e_1 - e_3$ for E7 as $+(9.3 \pm 0.3) \times 10^{-12}$ Cm^{-1}, and for E70A as $+(3.5 \pm 0.2) \times 10^{-12}$ Cm^{-1}. However, by using a conoscopic technique, and therefore simultaneously measuring the transmission at all angles of incidence within a cone, a greater amount of data can be gathered and used in the measurement.

In order to interpret the conoscopic images obtained, they are compared with theoretically predicted images. These are generated for each director profile using an extended Jones technique [10, 11] to find the transmitted intensity between crossed polarisers at a range of angles of incidence (both polar and azimuthal). A simple Matlab code is used to generate a conoscopic image from this output. For example, Figure 2 shows the predicted conoscopic image (using a red HeNe laser wavelength of 632.8nm) for a 100μm thick TN cell under various applied electric fields. Part (a) shows the image for no applied field in the case where the polarisers are oriented at $\pm 45^\circ$ to the rubbing directions. Part (b) shows the predicted image for a field of 0.01V/μm, but with the flexoelectric coefficient set to zero in the model. The image is essentially a rotated version of the zero volts image, corresponding to the pure twist in the director profile. Parts (c) and (d), however, show the predicted conoscopic images when flexoelectricity is included in the model for both positive and negative applied fields. Note that now not only is there a rotation compared to zero volts, but there is a shift in the centre of the conoscopic image, and that this is in opposite directions for the two signs of applied field. This shift is caused by the tilt in the director profile seen in Figure 1 (a).

By comparing the predicted conoscopic images for different values of the flexoelectric coefficient with those measured experimentally, it is possible to determine a value for the flexoelectric coefficient. Therefore, in the theoretical modelling, this parameter is treated as unknown. The exact thickness of the device, and the constant of proportionality between the electric field and the applied voltage are also treated as unknowns. Although the cell thickness can be measured before

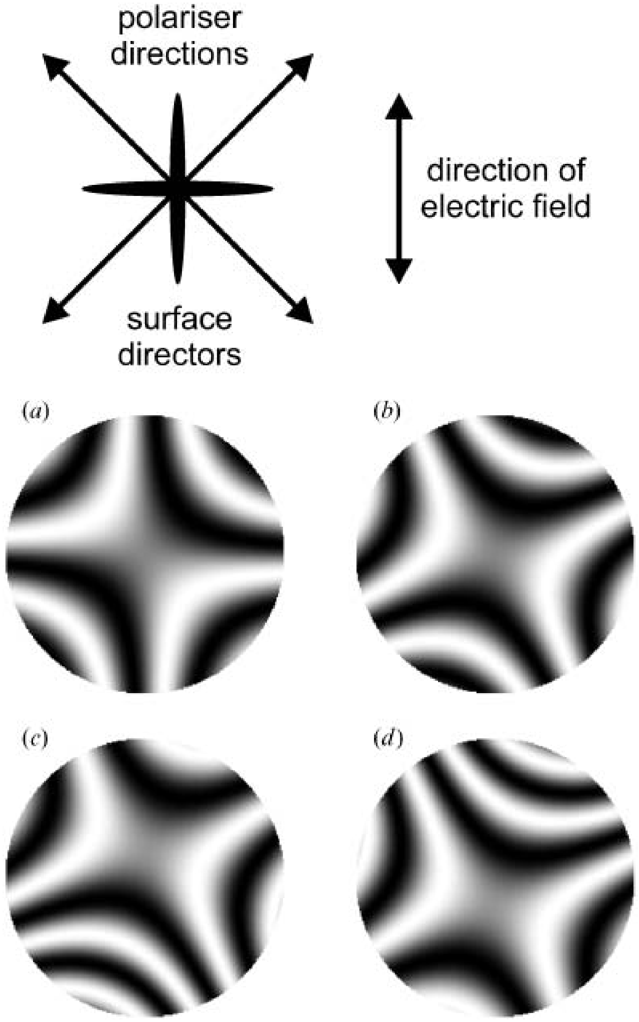

Figure 2. Theoretically predicted conoscopic images generated using the director profiles shown in Figure 1, together with an extended Jones optical technique: (a) the ground state, (b) an applied in-plane electric field of $\pm 0.01 V/\mu m$, with no flexoelectric coupling, (c) and (d) the same magnitude of electric field with $e_1 - e_3 = 10.0 \times 10^{-12} Cm^{-1}$, and equal and opposite fields for (c) and (d).

Table 1. Table showing the fixed parameter values for E7 used in the theoretical model in this work

K_{11}	11.1pN
K_{22}	6.5pN
K_{33}	17.1pN
$\Delta\varepsilon$	14.3
Δn	0.22

filling the cell using an interferometric technique, it is well known to change slightly on filling, and will depend weakly on position in the cell. We therefore use the zero volts experimental conoscopic image to determine the exact thickness of the device at the point of measurement. Similarly, the electric field in the electrode gap is not simply $E = V/g$, where V is the applied voltage and g is the electrode gap, but is usually around a factor of 0.6–0.8 less than that. The exact value is determined by the dielectric constant of the liquid crystal and the position within the electrode gap. We determine this factor by using high frequency measurements, in which the liquid crystal can only respond to the rms electric field, and will therefore not tilt due to the flexoelectric effect. By comparing these images with those generated theoretically using zero flexoelectric coefficient, the constant of proportionality between E and V can be determined. The remaining parameters in the model (elastic and dielectric constants and refractive indices) are well known for the material under consideration (E7) and are therefore kept constant. These values are summarised in Table 1.

The experimental arrangement used to obtain the conoscopic images is shown in Figure 3. The cell is placed at the common focus of a pair of identical microscope objectives of numerical aperture 0.5. Incident on the first of these is an expanded beam of linearly polarised light from a HeNe laser (wavelength 632.8nm), the coherence of the beam having been broken by a rotating diffuser. A charged coupled device

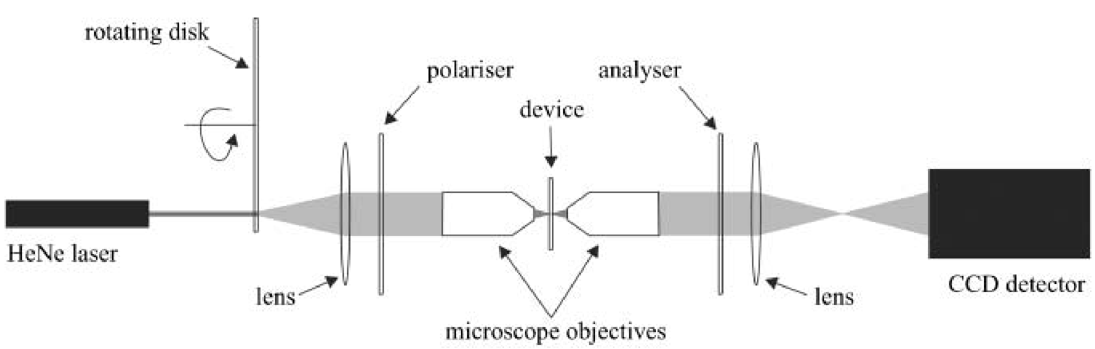

Figure 3. Illustration of the experimental arrangement used to obtain the conoscopic images. The cell is illuminated with a cone of linearly polarised light whose coherence has been broken by a rotating diffuser. The conoscopic image is collected, via an analyser crossed with the input polariser, by a CCD camera.

(CCD) detector collects the output from the second objective through an analyser crossed with the input polariser. This optical arrangement therefore collects simultaneously the transmittance of the device between crossed polarisers for a range of incident angles up to a maximum radial angle of 30° in air, as determined by the numerical aperture of the objectives.

The cell used is a thick (≈100μm) twisted nematic cell made with two glass substrates which coated are with a thin layer of PVA, rubbed to produce very low pretilt (<1°) homogeneous alignment. In order to apply an in-plane electric field, one of the glass substrates (coated in ITO) has a rectangular gap etched away down the centre. The other substrate has no ITO layer. The electrode gap is 500μm wide in this case: wide enough that we can make optical observations inside the gap, and also so that in combination with a device thickness of 100μm, the electric field can be considered to be parallel to the glass plates. The cell is filled with nematic mixture E7 from Merck.

The conoscopic images obtained experimentally for this device are shown in Figure 4. Part (a) shows the zero volts image, part (b) shows an example of an image taken with a high frequency square wave applied (20V rms across the 500μm electrode gap), and parts (c) and (d) show images taken with a 5V low frequency square wave applied for both the positive and negative parts of the voltage cycle.

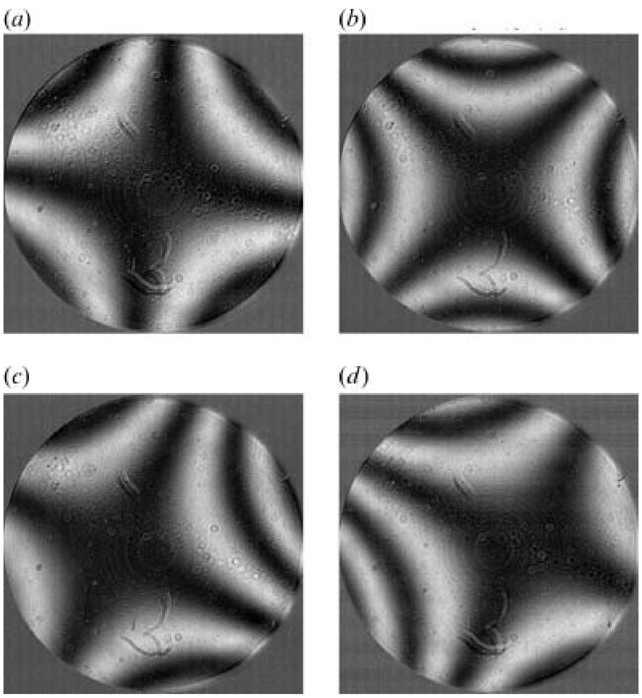

Figure 4. Experimental conoscopic images for a twisted nematic cell: (a) in the ground state, (b) under the application of a high frequency square wave of amplitude 20V (across a gap of 500μm), (c) and (d) under dc voltages of $\pm$5V respectively.

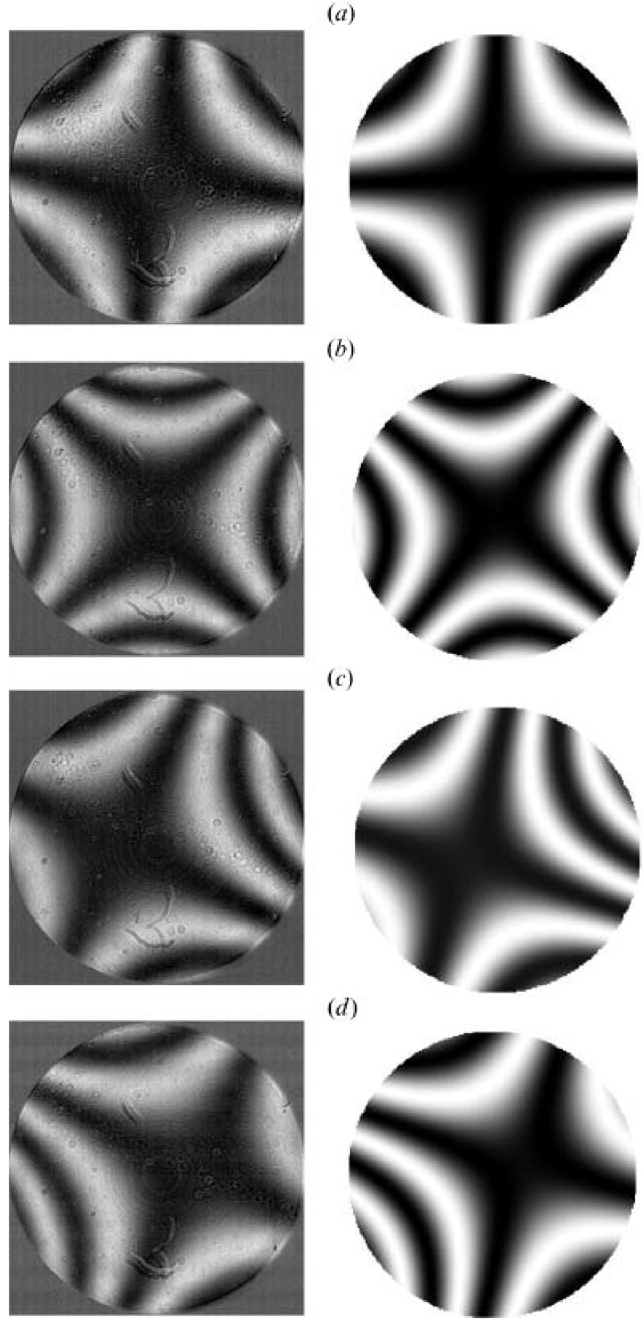

Figure 5. Comparison of the experimental results of Figure 4 (left hand column) with the best fit theoretical simulations (right hand column). For the theoretical images, part (a) is for zero applied voltage, part (b) is for 20V with no flexoelectric coupling, and parts (c) and (d) are for 5V and a flexoelectric parameter of $e_1 - e_3 = 9.0 \times 10^{-12}$Cm^{-1}.

For a range of applied voltages, a comparison of high frequency experimental results with conoscopic images predicted with zero flexoelectric coefficient resulted in the following relationship between the applied voltage V and the electric field inside the cell E:

$$E = 0.70\frac{V}{g}, \quad (3)$$

where g is the electrode gap, i.e. 500μm in this case. Both the zero volts image and the high frequency applied voltages were consistent with a device thickness used in the theoretical model of 95.5μm. Using this device thickness and relationship between E and V, a comparison was made between low frequency images obtained experimentally and conoscopic figures generated theoretically using a variable flexoelectric coefficient. In order to compare experimental and theoretical images quantitatively, slices were taken through the conoscopic images, either at a constant azimuthal angle, or at a constant polar angle. The best value for the flexoelectric coefficient was then determined as that which gave the best match between theory and experiment. The error on that value was determined by the range of values of the flexoelectric coefficient that made no significant difference to the fitting. The best comparison between theory and experiment was found for a value of $e_1 - e_3 = +(9.0 \pm 1.0) \times 10^{-12}\mathrm{Cm}^{-1}$. As Figure 5 shows, the comparison is extremely good. We note that this value for the difference in the flexoelectric coefficients is consistent with our previous measurements in E7 [9].

To conclude, we have used a conoscopic technique to determine the difference of the flexoelectric coefficients $e_1 - e_3$ in the liquid crystal mixture E7. By comparing experimental and theoretical results for TN cells with in-plane electric fields, we have found that the value is $+(9.0 \pm 1.0) \times 10^{-12}\mathrm{Cm}^{-1}$. Although there is a greater amount of data taken with this conoscopic technique, it is less accurate than the two-beam method [9] overall because of the uncertainty in relating position within the conoscopic image to the angle of incidence through the cell. However, the experiment is useful in that it shows the 'whole picture' in terms of the transmission of a TN cell as a function of angle of incidence, in which our two beam method corresponds to two points. As such, the conoscopic images provide a striking illustration of the strength of flexoelectric effects in nematic liquid crystals.

LAP-J would like to acknowledge the financial support of the Royal Society for this work.

References

[1] R.B. Meyer. *Phys. Rev. Lett., 22* 18, pp. 918 (1969).
[2] J.S. Patel, R.B. Meyer. *Phys. Rev. Lett.*, **58**, 15, pp. 1538 (1987).
[3] P. Rudquist, L. Komitov, S. Lagerwall. *Phys. Rev. E, 50* 6, pp. R4735 (1994).
[4] H.J. Coles, B. Musgrave, M.J. Coles, J. Willmott. *J. Mater. Chem, 11* 11, pp. 2709 (2001).
[5] G.P. Bryan-Brown, E.L. Wood, C.V. Brown, J.C. Jones, I.C. Sage, P. Brett. *proc. IDW '97*, pp. 261 (1997).
[6] G.P. Bryan-Brown, C.V. Brown, J.C. Jones, E.L. Wood, I.C. Sage, P. Brett, J. Rudin. *SID 97 Digest*, **28**, pp. 37 (1997).
[7] A.G. Petrov. *Measurement and Interpretation of Flexoelectricity*, chapter in the book *Physical Properties of Liquid Crystals: Nematics* edited by D.A. Dunmar, A. Fukuda, G.R. Luckhurst (Eds)published by INSPEC (2001).
[8] L.A. Parry-Jones, S.J. Elston. *J. Appl. Phys.*, **97**, 093515 (2005).
[9] R. Ewings, C. Kischka, L.A. Parry-Jones, S.J. Elston. *Phys. Rev. E*, **73**, 011713 (2006).
[10] C. Gu, P. Yeh. *Displays*, **20**, pp. 237 (1999).
[11] L.A. Parry-Jones, E. Kriezis, S.J. Elston. *Jpn. J. Appl. Phys.*, **41**, pp. L1485 (2002).